AD-A035 029 AIR FORCE MATERIALS LAB WRIGHT-PATTERSON AFB OHIO F/G 11/6
THE EFFECT OF GRAPHITE-EPOXY COMPOSITES ON THE GALVANIC CORROSI--ETC(U)
SEP 76 B A MILLER, S G LEE

UNCLASSIFIED AFML-TR-76-121 NL

| OF |
AD
A035029

END

DATE
FILMED
3-77

AFML-TR-76-121

THE EFFECT OF GRAPHITE-EPOXY COMPOSITES ON THE GALVANIC CORROSION OF AEROSPACE ALLOYS

AERONAUTICAL SYSTEMS BRANCH
SYSTEMS SUPPORT DIVISION

SEPTEMBER 1976

TECHNICAL REPORT AFML-TR-76-121
FINAL REPORT FOR PERIOD 1 JANUARY 1975 - 1 APRIL 1976

AIR FORCE MATERIALS LABORATORY
AIR FORCE WRIGHT AERONAUTICAL LABORATORIES
AIR FORCE SYSTEMS COMMAND
WRIGHT-PATTERSON AIR FORCE BASE, OHIO 45433

NOTICE

When Government drawings, specifications, or other data are used for any purpose other than in connection with a definitely related Government procurement operation, the United States Government thereby incurs no responsibility nor any obligation whatsoever; and the fact that the government may have formulated, furnished, or in any way supplied the said drawings, specifications, or other data, is not to be regarded by implication or otherwise as in any manner licensing the holder or any other person or corporation, or conveying any rights or permission to manufacture, use, or sell any patented invention that may in any way be related thereto.

This report has been reviewed by the Information Office (IO) and is releasable to the National Technical Information Service (NTIS). At NTIS, it will be available to the general public including foreign nations.

This technical report has been reviewed and is approved for publication.

Fred H. Meyer

FRED H. MEYER, Jr.
Project Engineer

FOR THE COMMANDER

Thomas D. Cooper

THOMAS D. COOPER, Chief
Aeronautical Systems Branch
Systems Support Division

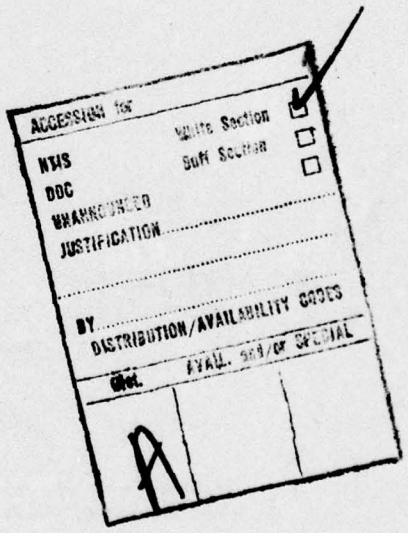

Copies of this report should not be returned unless return is required by security considerations, contractual obligations, or notice on a specific document.

AIR FORCE - 29 DECEMBER 76 - 150

UNCLASSIFIED
SECURITY CLASSIFICATION OF THIS PAGE (When Data Entered)

REPORT DOCUMENTATION PAGE

READ INSTRUCTIONS BEFORE COMPLETING FORM

1. REPORT NUMBER: AFML-TR-76-121
2. GOVT ACCESSION NO.
3. RECIPIENT'S CATALOG NUMBER
4. TITLE (and Subtitle): THE EFFECT OF GRAPHITE-EPOXY COMPOSITES ON THE GALVANIC CORROSION OF AEROSPACE ALLOYS.
5. TYPE OF REPORT & PERIOD COVERED: Final Report, 1 January 75- 1 April 1976
6. PERFORMING ORG. REPORT NUMBER
7. AUTHOR(s): BENNIE A. MILLER, Capt, USAF; SYLVESTER G. LEE
8. CONTRACT OR GRANT NUMBER(s)
9. PERFORMING ORGANIZATION NAME AND ADDRESS: Air Force Institute of Technology, Wright-Patterson Air Force Base, OH 45433
10. PROGRAM ELEMENT, PROJECT, TASK AREA & WORK UNIT NUMBERS
11. CONTROLLING OFFICE NAME AND ADDRESS: Air Force Materials Laboratory, Wright-Patterson Air Force Base, OH 45433
12. REPORT DATE: September 1976
13. NUMBER OF PAGES: 47
14. MONITORING AGENCY NAME & ADDRESS (if different from Controlling Office): 45p.
15. SECURITY CLASS. (of this report): UNCLASSIFIED
15a. DECLASSIFICATION/DOWNGRADING SCHEDULE
16. DISTRIBUTION STATEMENT (of this Report): Approved for public release; distribution unlimited.
17. DISTRIBUTION STATEMENT (of the abstract entered in Block 20, if different from Report)
18. SUPPLEMENTARY NOTES
19. KEY WORDS (Continue on reverse side if necessary and identify by block number): Graphite-epoxy Composites; Galvanic Corrosion
20. ABSTRACT (Continue on reverse side if necessary and identify by block number):

The galvanic corrosion rates of selected aerospace alloys coupled to graphite-epoxy composite materials (GECM) in aerated neutral (pH7) 3.5% NaCl at 22+1°C have been studied. Galvanic current was measured by the use of a potentiostat modified to operate as a zero-resistance ammeter (ZRA). Weight-loss tests were also conducted. Four types of GECM were used along with pure graphite. Twenty-three alloys, including steels, stainless steels, aluminum, berylium-copper, nickel-base, and titanium alloys, were → over

DD FORM 1 JAN 73 1473 EDITION OF 1 NOV 65 IS OBSOLETE

UNCLASSIFIED
SECURITY CLASSIFICATION OF THIS PAGE (When Data Entered)

012320

tested for galvanic compatibility with GECM.

Conclusions derived from the results of this study were: (1) galvanic series based upon potentials are a poor indicator of GECM/alloy galvanic corrosion; (2) monitoring of galvanic current indicates the time dependent variations of galvanic current better than weight-loss tests; (3) aluminum alloys and steels are least compatible with GECM, stainless steels and Be-Cu are more compatible, and nickel-base and titanium alloys show excellent compatibility; (4) based on the arbitrary criterion of magnitude of galvanic current density the acceptability by particular alloy is as follows: Acceptable - Ti-6Al-4V, Ti-6Al-2Sn-4Zr-2Mo, René 41, Inconel X, Inconel, AFC-77, PH 17-7, SS-304, Be-Cu, SS-301. Borderline - Aluminum-Graphite Composite, MA-87, SS-440C, Al-2024-T6, Al-2024-T3, 1020, Al-7075-T6, 4130. Unacceptable - AF 1410, 300M, Al-2020-T651, and 4340; (5) The effect of different types of GEC material on the galvanic corrosion current of alloys is minimal; and (6) Galvanic current data were shown to agree with estimates of galvanic compatibility from other experiments, such as salt-spray and long-term atmospheric tests.

FOREWORD

This report is based in part on thesis research performed by Capt. B. A. Miller while a graduate student at AFIT in collaboration with the coauthor.

The authors gratefully acknowledge the encouragement and suggestions provided by Lt. Peter F. Dexter (AFFDL-FEM). The support of Lt. Col. James A. Snide (AFML-MX) and Dr. James R. Myers (AFIT-DE) throughout this study is also appreciated.

TABLE OF CONTENTS

SECTION		PAGE
I	INTRODUCTION	1
	1. Purpose	1
	2. Background	2
II	RELATIONSHIP OF GALVANIC CURRENT TO ANODIC DISSOLUTION RATE	5
III	ELECTROCHEMICAL PROPERTIES OF GRAPHITE	10
IV	PREVIOUS STUDIES OF GECM/ALLOY COUPLES	12
V	EXPERIMENTAL PROCEDURE	14
	1. Materials	14
	2. Specimens	16
	3. Open-Circuit Potentials and Potential Difference Measurements	16
	4. Galvanic Current Measurements	17
VI	RESULTS	22
	1. Corrosion Potential Measurements	22
	2. Galvanic Current Data	23
VII	DISCUSSION	28
	1. Alloy Behavior	28
	2. Potential vs Galvanic Current for Galvanic Corrosion Estimates	30
	a. Acceptability Criteria	31
	b. Correlation of Average Galvanic Current Density and Galvanic Corrosion Determined From Weight-Loss Tests	31
	3. Galvanic Current Data vs Accelerated and Long-Term Tests on Actual GECM/Alloy Joints	33
VIII	CONCLUSIONS	35
REFERENCES		36

LIST OF TABLES

TABLE		PAGE
1	Aerospace Structures Fabricated or Proposed for Fabrication from Graphite Epoxy Composite Material	3
2	Uncoupled Potentials vs SCE Determined by Johnston et al (Reference 6)	13
3	Graphite Epoxy Composite Materials (GECM) Tested, Including Manufacturer, Short Description, and Number Samples of Each Tested, Along with Pure Graphite	14
4	Composition of Alloy Tested in Nominal Weight Percent	15
5	Corrosion Potentials Before (ϕ^{s}_{corr}) and After (ϕ^{e}_{corr}) Galvanic Couple Test, 3.5% NaCl, pH 7, 22 ± 1°C	20
6	Open Circuit Corrosion Potential (ϕ_{corr}) After 24 Hrs in 3.5% NaCl, Corrosion Potentials Before (ϕ_{corr}), and After (ϕ_{corr}) Galvanic Couple Test for Graphite Materials, 3.5% NaCl, pH7, 22 ± 1°C	23
7	Galvanic Series for GECM Coupled with Aluminum Alloys in 3.5% NaCl	24
8	Galvanic Series for GECM Coupled with Steels in 3.5% NaCl	25
9	Galvanic Series for GECM Coupled with Stainless Steels in 3.5% NaCl	26
10	Galvanic Series for GECM Coupled with Nickel-Base Alloys in 3.5% NaCl	26
11	Galvanic Series for GECM Coupled with Titanium Alloys and Be-Cu in 3.5% NaCl	27
12	Galvanic Series for GECM Based on Average Current Density $\bar{i}_g$ in 3.5% NaCl	30
13	Acceptability Criteria for Alloys Tested	32

LIST OF ILLUSTRATIONS

FIGURE		PAGE
1	Evans (Polarization) Diagrams Showing Types of Control	7
2	Polarization Curves Showing Galvanic Current When Steel is Coupled to Titanium or Copper in Seawater (References 4, 19)	11
3	Circuit Diagram of Potentiostat Zero-Resistance Ammeter Used to Measure Galvanic Current with the Galvanic Cell Represented by its Electrical Equivalent	18
4	Schematic of Potentiostat Zero-Resistance Ammeter Used in Measuring Galvanic Current	18
5	Typical Time vs I_g Curves for the Indicated Alloys vs GECM	19

SUMMARY

Graphite-epoxy composite materials (GECM) exhibit many properties that make them desirable for use in aerospace applications. These include high elastic modulus, high strength-to-weight ratio, and good corrosion resistance. However, in many applications GECM must be used in intimate contact with metallic components. This is necessary because GECM is inferior to metals for use as bushings, bearings, and fasteners. The deleterious effect of graphite marking pencils and graphite-base lubricants in promoting the galvanic corrosion of aluminum and aluminum alloys in the Air Force is well documented (Reference 7).

Previous studies have shown that GECM also accelerates the corrosion of less noble materials (e.g., aluminum alloys, cadmium-plated steel) when galvanically coupled. It is evident then that there is a potentially serious risk of galvanic corrosion whenever GECM are coupled to certain alloys.

Since earlier reports on the galvanic corrosion of GECM-metal couples were limited to only a few alloys and did not report on the variation of galvanic corrosion current with time, it was felt that the present work would contribute to the basic understanding of this potential galvanic corrosion problem.

A controlled laboratory study was made of the galvanic corrosion that occurs when GECM are coupled with various alloys in neutral 3.5% aqueous NaCl at room temperature. These tests simulated GECM alloy joints that occur in aerospace applications. Several alloy types were considered, including steels, stainless steels, nickel-base, copper-base, aluminum, and titanium alloys. Four types of GECM were used along with pure graphite. Twenty-three alloys were tested for compatibility with GECM. Electrochemical test methods included potential measurements and galvanic current measurements. Galvanic current was measured by the use of potentiostat modified to operate as a zero-resistance ammeter. Weight-loss tests were also conducted.

Conclusions derived from the results of this study are: (1) galvanic series based upon potentials are a poor indicator of GECM/alloy galvanic corrosion; (2) monitoring of galvanic current indicates the time dependent variations of galvanic current better than weight-loss tests; (3) aluminum alloys and steels are least compatible with GECM, stainless steels and Be-Cu are more compatible, and nickel-base and titanium alloys show excellent compatibility; (4) based on the arbitrary criterion of magnitude of galvanic current density the acceptability by particular alloy is as follows: Acceptable - Ti-6Al-4V, Ti-6Al-2Sn-4Zr-2Mo, Rene' 41, Inconel X, Inconel, AFC-77, PH 17-7, SS-304, Be-Cu, SS-301. Borderline - Aluminum-Graphite Composite, MA-87, SS-440C, Al-2024-T6, Al-2024-T3, 1020, Al-7075-T6, 4130. Unacceptable - AF 1410, 300M, Al-2020-T651, and 4340; (5) the effect of different types of GEC material on the galvanic corrosion current of alloys is minimal; and (6) galvanic current data were shown to agree with estimates of galvanic compatibility from other experiments, such as salt-spray and long-term atmospheric tests.

SECTION I

INTRODUCTION

1. PURPOSE

The purpose of this investigation was to study the galvanic corrosion that occurs when an alloy is coupled with Graphite-Epoxy Composite Material (GECM) in contact with an electrolyte. An anticipated application of the results of this study would be the provision of a guideline to be used in the selection of fastener or bearing alloys to be coupled with GECM. Four types of GECM were used as a basis for tests to determine any variations in the corrosion properties among the different composites. Pure graphite samples were also tested to determine whether GECM corrosion properties are similar to those of pure graphite.

Alloys investigated included several that are commonly used on aircraft and space structures and a few that are proposed for aerospace application. Specifically, alloys from the following major alloy types were evaluated: (1) aluminum alloys, (2) steels, (3) stainless steels, (4) titanium alloys, (5) nickel-base alloys, and (6) beryllium copper.

The electrolyte (corrosive medium) used for galvanic testing was aerated 3.5% sodium chloride (NaCl) at room temperature (22 ± 1°C). This electrolyte composition was chosen for three reasons. First, it simulates the NaCl content of natural seawater. Second, it has been found that iron and steel alloys have their highest corrosion rate in this NaCl concentration (Reference 1). Finally, a large number of investigators have used this electrolyte in other corrosion studies; thus results of the present study could be used to complement the earlier data.

Immersion of the alloy/GECM couple in 3.5% NaCl and the use of electrochemical experimental apparatus produced data which were tabulated according to the couples' corrosion resistance. These data also indicated the variation of galvanic corrosion parameters with time.

The method selected for collecting galvanic corrosion data was the use of a potentiostat modified to operate as a zero resistance ammeter (ZRA). This electrochemical method was chosen because it allows measurement of very small currents with minimum error while minimizing any crevice corrosion effects. The method also reduced the test duration by making possible the evaluation of several couples in a relatively short time.

2. BACKGROUND

Graphite-epoxy composite material is one of the relatively new materials known as advanced composites. Its existence is due to the technological progress made in the nonmetallic materials field during the last decade. The composite is composed of high strength, high modulus graphite fibers combined with an amine-cured epoxy resin (Reference 2). The graphite fiber is produced by heating polyacrylonitrile (PAN) in air and then carbonizing it in an inert atmosphere at a much higher temperature. The process produces continuous filament bundles of graphite fiber which can be woven, twisted, or chopped and then impregnated with selected epoxy resins to form various shapes such as sheets, tubes, and even extruded structural members.

The primary advantage of GECM for aerospace applications is its high strength to weight ratio (Reference 2). Weight savings of 25% to 50% have been demonstrated on aircraft components. For example, on the A-37B aircraft main landing gear side brace, the GECM replacement part withstood ultimate loads and endured the required four fatigue lifetimes with a weight reduction of 35% over the aluminum-alloy part (Reference 3). Several applications of GECM on operational aerospace components and proposed applications are listed in Table 1.

Because of its high strength to weight ratio, GECM is being considered for many aerospace components. Some potentially disadvantageous properties have been noted, one of which is the subject of this report.

TABLE 1

AEROSPACE STRUCTURES FABRICATED OR PROPOSED FOR
FABRICATION FROM GRAPHITE EPOXY COMPOSITE MATERIALS

Technically Demonstrated	Current Production	Proposed
F-5 Wing Tip	F-111 Underwing Fairing	B-1 Horizontal Stabilizer
F-5 Landing Gear Door	F-15 Rudders	B-1 Weapon Bay Doors
F-5 Leading Edge Flap	F-15 Vertical Stabilizer Leading Edge	B-1 Vertical Stabilizer
F-5 Horizontal Stabilizer	F-16 Horizontal Stabilizer	B-1 Landing Gear Door
F-5 Trailing Edge Flap	F-16 Vertical Stabilizer	F-18 Wing Skins
A-7 Outer Wing Panels	F-16 Rudder	F-18 Empennage
737 Spoilers	Space Shuttle Cargo Doors	DC-10 Rudder
F-111 Fuselage (Aft)		F-15 Elevator Structure
F-5 Fuselage (Aft)		
YF-16 Fuselage (Fwd)		
A-37B Landing Gear Side Braces		

Graphite behaves electrochemically like a noble metal such as gold or platinum, and, accordingly, exhibits a noble potential in most electrolytes. This suggests that this material will be cathodic to most metals upon galvanic coupling; a less noble metal would be expected to corrode due to the potential difference. It is important to note that whether or not corrosion of the anode occurs is dependent on kinetic parameters, such as exchange current density of the cathodic reduction reaction, uncoupled corrosion rates, and area ratios as well as potential difference between the cathodic and anodic members of the galvanic couple (Reference 4).

Galvanic corrosion of aluminum alloys has occurred on aircraft parts when the corrosive medium is either tapwater (Reference 5) or seawater (Reference 6). Additionally, the deleterious effect of graphite marking pencils and graphite-base lubricants in promoting the galvanic corrosion of aluminum and aluminum alloys in the aircraft industry is well documented (Reference 7). Because of the potential for galvanic corrosion, an important consideration in component design where GECM is a proposed material would be the compatibility of GECM with various alloys used in fabrication. This research was conducted to determine the effect of GECM on the corrosion rates of various alloys coupled to this material.

SECTION II

RELATIONSHIP OF GALVANIC CURRENT TO ANODIC DISSOLUTION RATE

Galvanic corrosion is one of the most frequently encountered and severe types of corrosion. Prior to about 1970, when Mansfeld began publication of numerous papers on the phenomenon (Reference 8), very little research on the theory of galvanic corrosion had been reported. The results of these studies are pertinent to the interpretation of the data presented in this report, and, therefore, will be summarized.

Mansfeld pointed out that the magnitude of galvanic corrosion depends not only on the potential difference of dissimilar metals, but also on kinetic parameters such as corrosion rates of the uncoupled materials, Tafel slopes and on area ratios (Reference 9). It has been shown, using the mixed potential theory, that there exists a relationship between galvanic current and dissolution (corrosion) rates of the anodic half of galvanic couples, but that the functional relationship varies with different conditions of polarization and control (Reference 9). For the sake of organization and clarity three different cases were considered. In the first case, the galvanic potential (ϕ_g) is so far removed from the open-circuit (corrosion) potential of either of the uncoupled electrodes that only a reduction reaction occurs on the cathode and only an oxidation reaction occurs on the anode; this is shown in the Evans diagram in Figure 1(a). If Tafel behavior is observed and charge transfer occurs in the reactions, then the measured galvanic current (I_g) equals the dissolution current (I_d) for the anode.

$$I_g = I_d \tag{1}$$

In this situation weight-loss data should agree with galvanic current data. When the polarization of the anode due to galvanic coupling is small, case two exists. Here the anode remains in the region of mixed potentials so that a reduction as well as an oxidation reaction occurs on its surface

while only a reduction reaction takes place on the cathode, Figure 1 (b). Accordingly, the galvanic current I_g is related to the dissolution current (I_d) by

$$I_g = I_d - I^A_{corr} \exp\left(\frac{\phi_g - \phi^A_{corr}}{0.434\ b_c}\right) \tag{2}$$

where I^A_{corr} and ϕ^A_{corr} are corrosion current and corrosion potential of the anode, and b_c is the Tafel slope for the reduction reaction on the anode. If the polarization is small (i.e., $\phi^A_{corr} \simeq \phi_g$) the measured galvanic current approximates the increase in the dissolution current of the anode due to coupling to a more noble metal or material. In case three, Figure 1 (c), the reduction reaction at the cathode is under diffusion control; therefore, the corrosion current density (i^A_{corr}) of the anode is equal to the limiting current density $i^L_{O_2}$ for oxygen diffusion assuming a neutral aerated solution:

$$i^A_{corr} = i^L_{O_2} \tag{3}$$

The anodic dissolution current density, i^A_a was shown to equal

$$i^A_a = i^L_{O_2}\left(1 + \frac{A^C}{A^A}\right) = i^A_{corr}\left(1 + \frac{A^C}{A^A}\right) \tag{4}$$

which was described by Mansfeld as the "catchment area principle" earlier demonstrated in a classic paper by Whitman and Russell (Reference 10). For equal areas of anode and cathode this equation states that the corrosion rate of the anode in a galvanic couple under cathode diffusion control is equal to twice its uncoupled corrosion rate.

Galvanic current (I_g), the quantity measured in this study, is equal to the difference between the oxidation current (I^A_a) and the reduction current (I^A_c) of the anode at the short circuited or galvanic potential ϕ_g.

$$I_g = I^A_a - I^A_c \tag{5}$$

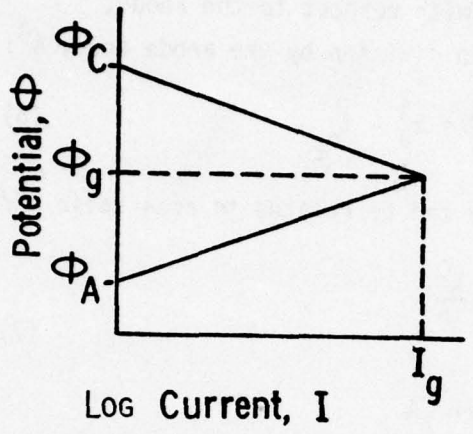

a. Case I, Mixed Control

$$I_g = I_d$$

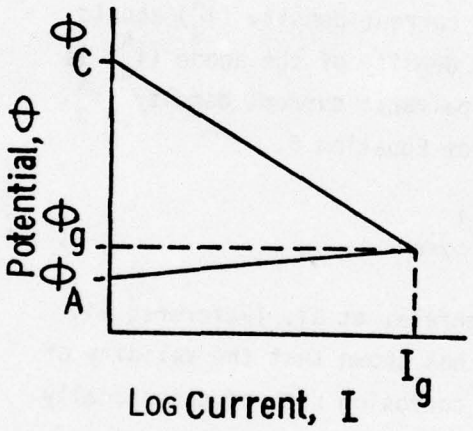

b. Case II, Cathodic Control

$$I_g = I_d - I^A_{corr} \exp\left(\frac{\phi_g - \phi^A_{corr}}{0.439\ b_c}\right)$$

if $\phi_g \simeq \phi^A_{corr}$

$$I_g = I_d - I^A_{corr}$$

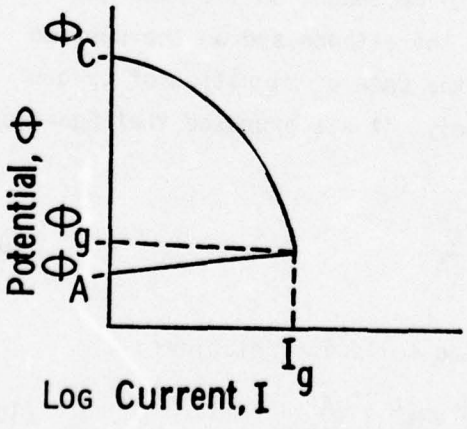

c. Case III, Diffusion Control

$$i^A_g = i^A_a - i^{L,A}_{o_2}$$

Figure 1. Evans (Polarization) Diagrams Showing Types of Control

Or in terms of galvanic current density with respect to the anode, Equation 5 converts to the following upon division by the anode area, A^A:

$$i_g^A = \frac{I_g}{A^A} = i_a^A - i_c^A = i_a^A - i_{o_2}^L \tag{6}$$

From Equation 4 galvanic current density can be related to area ratio A^C/A^A:

$$\begin{aligned} i_g^A &= i_{o_2}^L \frac{A^C}{A^A} \\ &= i_{corr}^A \frac{A^C}{A^A} \end{aligned} \tag{7}$$

for equal areas A^C and A^A, the galvanic current density (i_g^A) should be a constant. The dissolution current density of the anode (i_a^A) is related to the experimentally measured galvanic current density i_g^A by the following expressions derived from Equation 6.

$$i_a^A = i_g^A + i_{corr}^A \tag{8}$$

Experimental evidence presented by Rozenfeld, et al. (Reference 11) and Mansfeld and Parry (Reference 12), has shown that the validity of Equation 7 is questionable because the corrosion rate of galvanically coupled materials are not controlled solely by the diffusion rate of oxygen to the cathode surface but is also dependent on the exchange current density for oxygen reduction on the cathode and on the surface characteristics of the anode, such as, the rate of migration of oxygen through anodic surface films. Accordingly, it was proposed that Equation 7 be replaced by

$$i_g^A = i_{o_2}^{L,C} \frac{A^C}{A^A} \tag{9}$$

and that Equation 8 be substituted by the following relation:

$$i_a^A = i_g^A + i_{l_2}^{L,A} = i_g^A + i_{corr}^A \tag{10}$$

where in Equations 9 and 10 the material independent limiting diffusion current density $i^{L}_{o_2}$ has been replaced by the material dependent $i^{L,C}_{o_2}$ and $i^{L,A}_{o_2}$, respectively (Reference 4).

The preceding discussion was presented to show that galvanic current density (i^{A}_{g}), the quantity measured in this experiment, represents the increase in the dissolution rate of the anode coupled to Graphite-Epoxy Composite Material (GECM) and is therefore a valid quantity for use as a criterion for ranking alloys for galvanic compatibility with GECM.

SECTION III

ELECTROCHEMICAL PROPERTIES OF GRAPHITE

The galvanic current flowing between two coupled dissimilar metals in contact with an electrolyte, as discussed earlier, is a measure of the increase in corrosion rate due to coupling; this is the so-called "galvanic effect" (Reference 4). For the case of a relatively inert metal or material coupled to a less noble metal in aerated neutral media, such as seawater, the corrosion rate of the less noble material, the anode, is governed by the diffusion controlled rate of oxygen reduction on the more noble material, the cathode. The corrosion current then, cannot exceed a maximum value called the limiting diffusion current density, $i^L_{O_2}$. Its value depends on the efficiency at which the oxygen reduction reaction occurs on the cathode surface and is therefore a material dependent property. The difference in the magnitude of the galvanic current between steel-copper and steel-titanium couples is shown in Figure 2. The lower galvanic current for the Ti-steel couple I_{Ti} can be attributed to the fact that the oxide film (TiO_2) on titanium is a poor electronic conductor which inhibits the reduction reaction. On the other hand, copper is a more effective substrate for oxygen reduction with attendant higher galvanic current, I_{Cu} (References 4, 19).

Graphite has been used successfully as a reversible oxygen electrode for many years (Reference 13). This material is suitable for use as a substrate for the construction of oxygen electrodes because of its inertness, good electrical conductivity and because it is free from interfering oxide films such as those found on metals (Reference 14). This property explains the deleterious effect of galvanically coupling graphite or GECM to many metals.

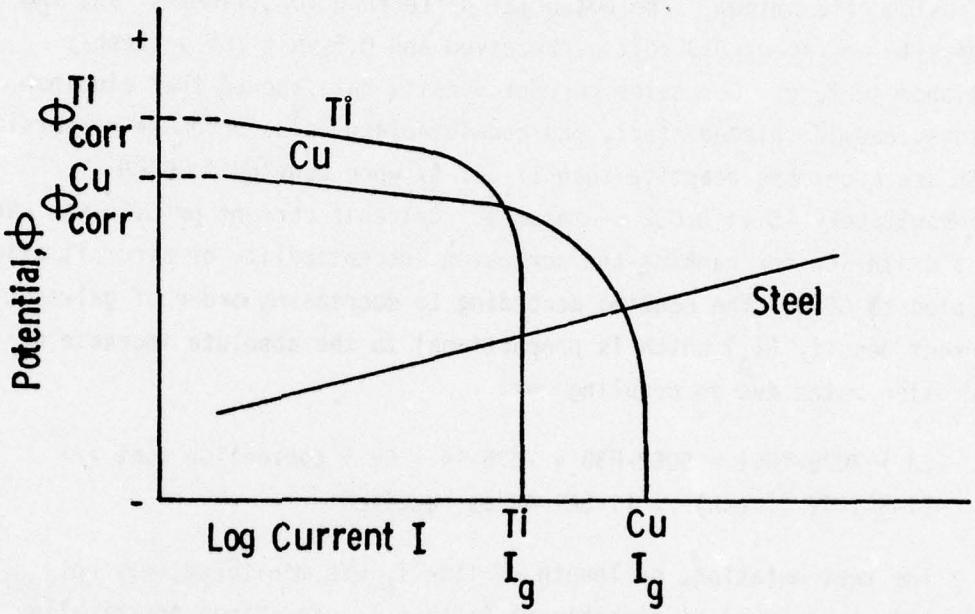

Figure 2. Polarization Curves Showing Galvanic Current When Steel is Coupled to Titanium or Copper in Seawater (References 4,19). Note limiting C.D. for reduction reaction is less for Ti than Cu.

SECTION IV

PREVIOUS STUDIES OF GECM/ALLOY COUPLES

Fischer and DeLuccia (Reference 15) conducted electrochemical tests to determine the nature of galvanic corrosion when GECM is coupled to aluminum, steel, and titanium alloys in neutral aerated 3.5% NaCl solution. Approximately one volt potential difference was found between the composite and 7075-T6 and 7075-T651 aluminum alloys. This relatively large potential provided the thermodynamic driving force for accelerated corrosion of aluminum. The potential difference for Ti-6Al-4V and the composite was about 0.3 volt as received and 0.5 volt for a freshly polished surface. Corrosion current density data showed that aluminum alloys, cadmium plated steel, and cadmium-plated plus chromate conversion coat are much more reactive than Ti-6Al-4V when coupled to GECM (approximately 15 vs 0.002 μ-amp/cm^2). Galvanic current or C.D. was used as a criterion for ranking the corrosion susceptibility of aircraft alloys coupled to GECM. The ranking according to decreasing order of galvanic current density (i_g) which is proportional to the absolute increase of corrosion rates due to coupling was:

Cd > 7075-T651 > 5052-H38 $\simeq$ 7075-T6 > Cd + conversion coat >>> Ti-6Al-4V (fresh) >> Ti-6Al-4V as received.

The test duration, or length of time I_g was monitored, was not reported; this could be significant in that I_g can change drastically with time (Reference 4).

Johnston and coworkers (Reference 6) also conducted electrochemical corrosion studies on GECM/alloy couples. Corrosion potentials of uncoupled GECM and various alloys versus Saturated Calomel Electrode (SCE) in aerated 3.5% NaCl solution are listed in Table 2.

Johnston also measured galvanic currents using the ZRA method discussed earlier. Galvanic current densities versus pH for several GECM/metal couples in one molar, air-saturated NaCl was reported. For pH7,

the values of i_g were: 400 μ-amp/cm^2 for GECM/Al, 200 μ-amp/cm^2 for GECM/Fe and 10 μ-amp/cm^2 for the GECM/Ti. Unfortunately, specific alloys were not designated, and also the test duration was not indicated.

TABLE 2

UNCOUPLED POTENTIALS VS SCE DETERMINED BY JOHNSTON, ET AL. (REFERENCE 6)

Material	E_{corr} (mv)
GECM	+ 120
Ti 6-4	- 420
4340 Steel	- 600
Al–7075–T6	- 780

Brown and Coomber (Reference 13) investigated the corrosion behavior of GECM/aluminum alloy galvanic couples in aqueous 5% NaCl. Corrosion potentials ϕ_{corr} for eight laboratory-prepared composites and one commercial composite were reported. The "steady-state" ϕ_{corr} for the commercial composite was about 50 mv positive to SCE; for all other (laboratory fabricated) composites, ϕ_{corr} was about 300 mv positive to SCE. Aluminum alloys were found to be about 600-700 mv negative to SCE.

Polarization studies showed that for GECM/aluminum alloy couples, polarization occurs almost exclusively at the GECM. The effects of chloride ion concentration, pH, temperature, oxygen concentration, and nature of cations and anions were studied with the following results: (1) the pH of the aqueous salt solution has little effect on polarization between pH 3 and 11, (2) rate of attack increases with temperature, but over the range of temperatures commonly found on aircraft components, the acceleration should not be of concern, (3) concentration of NaCl has only a small effect, (4) GECM acts as an oxygen electrode and the rate of attack on aluminum is proportional to the oxygen concentration of the electrolyte. It was concluded that aluminum alloys are susceptible to galvanic corrosion when coupled with graphite-epoxy composites.

SECTION V

EXPERIMENTAL PROCEDURE

1. MATERIALS

Graphite-epoxy composite materials tested in this study are listed in Table 3, along with a short description of the material, its manufacturer, and the number of samples tested.

Alloys tested and their nominal composition in weight precent are listed in Table 4. Experimental alloys that have been proposed for aerospace applications are Al-2020-T651, MA-87, AF 1410 steel, AFC-77 stainless steel, and aluminum-graphite (alloy-composite). Since very little corrosion testing has been accomplished on these alloys, the corrosion potential, and galvanic current data collected in this research should be of particular interest.

TABLE 3

GRAPHITE-EPOXY COMPOSITE MATERIALS (GECM) TESTED INCLUDING MANUFACTURER, SHORT DESCRIPTION, AND NUMBER SAMPLES OF EACH TESTED, ALONG WITH PURE GRAPHITE

Graphite Material	Manufacturer	Description	Number Tested
AS/3501-5	Hercules	Amine-cured epoxy resin reinforced with unidirectional graphite fibers.	44
Modmor	Narmco	Composed of layered 5206 tape with a modified epoxy resin system.	5
Magnamite	Hercules	Hercules AS fibers in an epoxy E-298 matrix.	2
T-300	Thornel	Graphite fibers impregnated with an epoxy specified as 5208.	4
Pure Graphite			5

TABLE 4

ALLOYS TESTED WITH NOMINAL COMPOSITION IN WEIGHT PERCENT

Test Alloys	Nominal Composition, Weight %
Al-2020-T651	4.5 Cu, 1.0 Li, 0.5 Mn, 0.2 Cd ---- Al
Al-7075-T6	5.6 Zn, 2.5 Mg, 1.6 Cu, 0.3 Cr ---- Al
MA-87 (P/M)	6.5 Zn, 2.5 Mg, 1.5 Cu, 0.4 Co ---- Al
Al-2024-T6,-T3	4.5 Cu, 1.5 Mg, 0.6 Mn ---- Al
Al Graphite	30.0 Graphite, 60.0 Al 6061 --- 1.0 Mg, 6.0 Si, 2.5 Cr, 2.25 Cu --- Al
4340 Steel	0.42 C, 0.75 Mn, 0.25 Si, 1.85 Ni, 0.82 Cr, 0.25 Mo, --- Fe
300M Steel	0.42 C, 1.85 Ni, 0.9 Cr, 5.0 Mo, 1.6 Si, 0.85 Mn --- Fe
AF 1410 Steel	2.0 Cr, 10.0 Ni, 14.0 Co, 1.0 Mo, 0.14 C --- Fe
4130 Steel	0.42 C, 0.95 Cr, 0.2 Mo, ---- Fe
1020 Steel	0.2 C ---- Fe
SS-440C	17.0 Cr, 0.5 Mo, High C --- Fe
SS-301	18.0 Cr, 8.0 Ni --- Fe
SS-304	19.0 Cr, 10.0 Ni, Low C --- Fe
SS-PH 17-7	.07 C, 17.0 Cr, 7.0 Ni, 1.2 Al --- Fe
SS AFC-77	0.15 C, 14.5 Cr, 13.0 Co, 5.0 Mo, 0.4 V --- Fe
Inconel	15.0 Cr, 7.0 Fe, --- Ni
Inconel X	15.0 Cr, 7.0 Fe, 2.5 Ti, 1.0 Co, 0.7 Al, --- Ni
Rene' 41	19.0 Cr, 11.0 Co, 10.0 Mo, 3.0 Ti, 1.5 Al, --- Ni
Ti-6Al-4V	6.0 Al, 4.0 V, ----- Ti
Ti-6Al-2Sn.....	6.0 Al, 2.0 Sn, 4.0 Zr, 2.0 Mo, ---- Ti
Be-Cu	1.74 Be ---- Cu

2. SPECIMENS

Corrosion test specimens were flat coupons 2.54 x 7.62 cm (1 x 3 inches) having various thicknesses. Alloy surfaces were wet ground with 120 grit SiC paper. GECM sample surfaces were tested in the as-received condition without any use of abrasives.

Lead wires (#12 or #14 insulated solid copper) were approximately 15 cm (6 in) long and were mechanically fixed to the sample by either of two methods. A fixed connection was chosen over the commonly used alligator clips because better contact could be made while eliminating current losses due to corrosion product build-up and accumulation of moisture at the lead-specimen interface. The first method consisted of top drilling a sample to a 0.635 cm (0.25 in) depth and friction forcing the lead into the hole for good electrical contact. The second method was used for samples too thin to top drill. In this case, a hole was drilled through the sample, and the flattened drilled lead wire was bolted to the sample. The lead-to-sample junctions for all specimens were first secured by the use of epoxy and subsequently top-coated with silicone elastomer to preclude moisture penetration and for electrical insulation.

The holder/spacer device consisted of two nylon bolts with nylon nuts, washers, and a 0.32 cm (0.125 in) spacer to separate the GECM and alloy surfaces and to keep them parallel. One bolt assembly was placed at the top of the sample and the other at the bottom. The bottom bolt prevented the samples from contacting the bottom of the test beaker. The spacers covered a very small portion of the total surface area; thus, crevice corrosion effects were minimized. Specimens were degreased in acetone and rinsed with distilled water, dried, and weighed to the nearest 0.1 mg before immersion in the 3.5% (by weight) NaCl test solution.

3. OPEN-CIRCUIT POTENTIALS AND POTENTIAL DIFFERENCE MEASUREMENTS

Corrosion potentials ϕ_{corr}, reference to SCE, for the uncoupled samples were measured using a high input impedance digital voltmeter (DVM).

Potential difference, $\Delta\phi_{corr}$ between GECM and an alloy was measured directly by using the DVM across the couple terminals.

4. GALVANIC CURRENT MEASUREMENTS

Galvanic current (I_g) was determined in this experiment by the use of a potentiostat modified to operate as a "zero resistance ammeter" (ZRA). This technique was first discussed by DeVay, Lenyel, and Meszaros in 1969 (Reference 16), and subsequently elaborated on by Von Fraunhofer and Banks (Reference 17).

The method of connecting the potentiostat to the galvanic cell when the instrument is applied as a ZRA is shown in Figures 3 and 4. Figure 3 represents the galvanic cell by its electrical equivalent. With the reference voltage set at zero, the potentiostat operates as a single-ended-inverting operational amplifier where the reference electrode terminal R. E. is at ground and is also a summing point.

Since the feedback current i_f equals i_{in}, the current flowing in the short-circuited galvanic cell, the cell current can be determined by measuring the output potential V_o between the working electrode W. E. (alloy) and the auxiliary electrode A. E. (GECM), and dividing this by the present resistance value of the feedback resistor R_f; i.e.,

$$i_f = I_g = \frac{V_o}{R_f} \tag{11}$$

This current was recorded over a 24-hour period using a high input impedance recorder. The resulting time - I_g plots were graphically integrated to determine $\bar{I}_g$, the average galvanic current. Typical time - I_g curves for steel, Al and titanium alloys versus GECM are shown in Figure 5. Note the variation of I_g with time. A computer program was used to reduce $\bar{I}_g$ data into average galvanic current density $\bar{i}_g$, and corrosion rates in milligrams per square-decimeter per day (mdd) and mils per year (mpy). Parameters other than $\bar{i}_g$ required for data reduction were: (1) alloy equivalent weight, (2) alloy density, (3) specimen planar area, and (4) test duration. Tables 5 through 12 list the reduced electrochemical data.

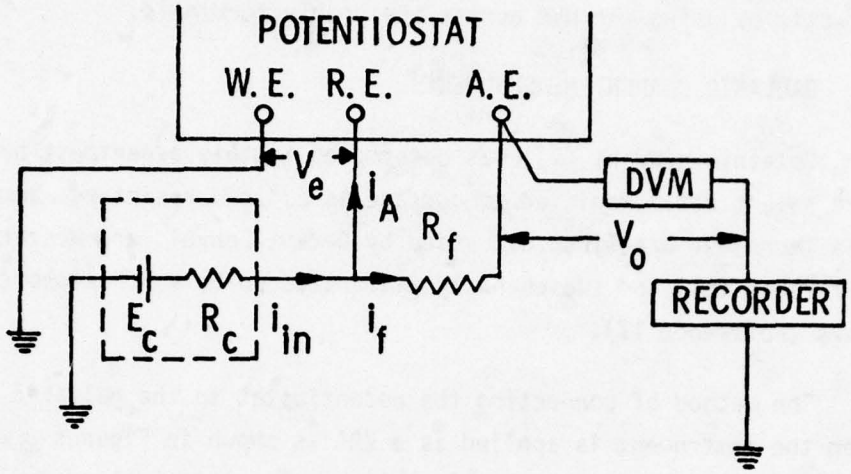

Figure 3. Circuit Diagram of Potentiostat ZRA Used to Measure Galvanic Current with the Galvanic Cell Represented by Its Electrical Equivalent

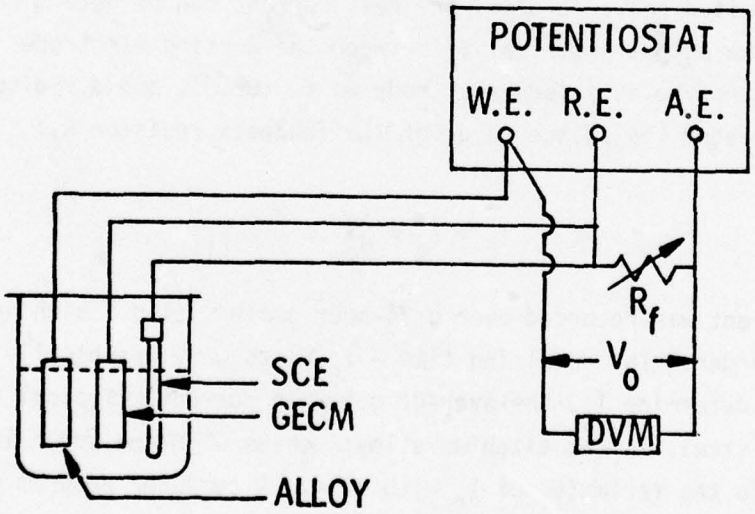

Figure 4. Schematic of Potentiostat ZRA Used in Measuring Galvanic Current

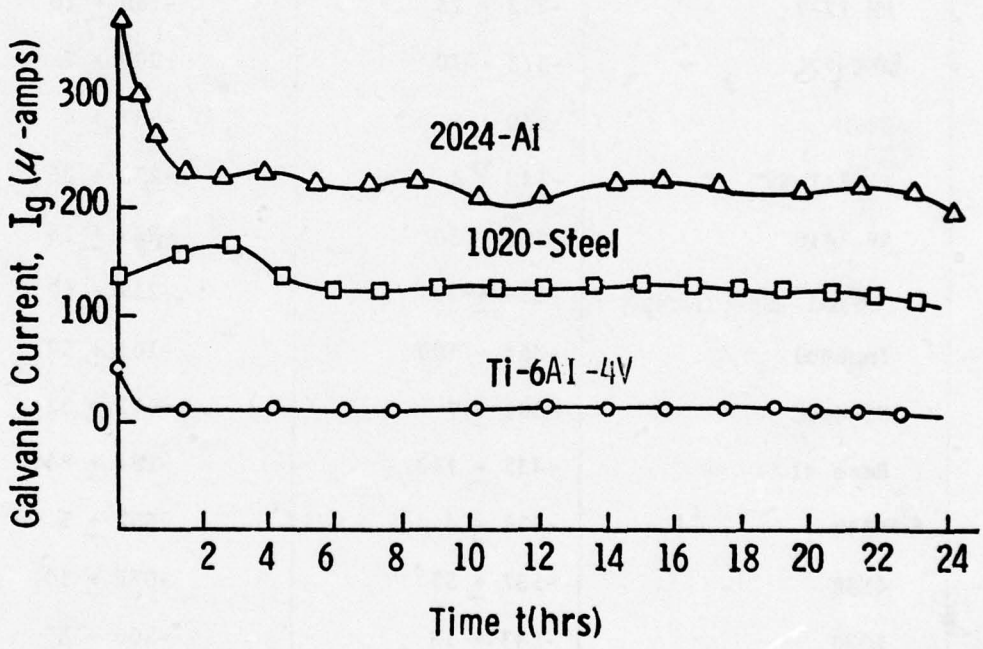

Figure 5. Typical Time vs I_g Curves for the Indicated Alloys vs GECM

TABLE 5

CORROSION POTENTIALS BEFORE (ϕ^{s}_{corr}) AND AFTER (ϕ^{e}_{corr})
GALVANIC COUPLE TEST, 3.5% NaCl, pH7, 22 + 1°C

Alloy	ϕ^{s}_{corr} (mv)	ϕ^{e}_{corr} (mv)
SS-301	-174 ± 65	-119 ± 76
Inconel X	-175 ± 25	-102 ± 10
SS-304	-210 ± 46	-109 ± 35
Be-Cu	-225 ± 5	-220 ± 5
PH 17-7	-252 ± 23	-139 ± 10
AFC-77	-318 ± 70	-209 ± 7
300M	-330 ± 5	-567 ± 4
Ti-6Al-4V	-343 ± 4	-270 ± 25
AF 1410	-358 ± 30	-529 ± 18
Ti-6Al-2Sn-4Zr-2Mo	-359 ± 29	-217 ± 69
Inconel	-364 + 100	-161 ± 57
SS-440C	-391 ± 7	-511 ± 32
Rene´ 41	-437 ± 110	-184 ± 84
4340	-534 ± 4	-667 ± 5
4130	-537 ± 55	-673 ± 10
1020	-543 ± 15	-566 ± 37
2024-T3	-652 ± 25	-783 ± 8
2024-T6	-656 ± 12	-753 ± 23
2020-T651	-724 ± 5	-821 ± 51
7075-T6	-775 ± 5	-751 ± 31
MA-87 (72)	-862 ± 3	-823 ± 7
MA-87 (73)	-868 ± 3	-849 ± 5
Aluminum Graphite	-868 ± 10	-808 ± 6

Actual weight-loss data, test duration, and the specimen area were used to calculate the dissolution rates, r_A, of the test specimen in mpy. The r_A values are also listed in Tables 8 through 12 as basis for comparison against corrosion rates determined from $\bar{i}_g$ data.

SECTION VI

RESULTS

1. CORROSION POTENTIAL MEASUREMENTS

The start and end test corrosion potentials (ϕ^s_{corr} and ϕ^e_{corr}) are listed in Tables 5 and 6. Values of ϕ^s_{corr} for the alloys (Table 5) are of interest because this list forms a galvanic series for aerated 3.5% NaCl solution at room temperature (22 ± 1°C) and pH7. The ranking in Table 5 lists the most noble alloy first, and descends in order to the most active alloy, or negative potential. As shown, stainless steels occupy the more noble potentials while aluminum alloys are most active. Although these data can be used for determining galvanic corrosion compatibility, it is decidedly inferior to the more reliable method of comparing the galvanic current produced by various GECM/alloy couples.

Comparing ϕ^s_{corr} and ϕ^e_{corr} of a given alloy suggests that the direction of potential change is indicative of the kinetic behavior of the alloy. It is noted, in general, that alloys with decreasing ϕ^s_{corr} versus ϕ^e_{corr} tend to have higher corrosion current than vice versa. For example, titanium alloys, nickel-base alloys, and most stainless steels have a ϕ^s_{corr} versus ϕ^e_{corr} that becomes more positive. These same alloys have low galvanic current. The opposite was true of most of the aluminum alloys and steels. These trends are closely related to the polarization effects or the kinetics of the galvanic reaction, and are thus more clearly shown when galvanic current is measured.

Table 6 lists potential, versus SCE, for the graphite materials tested. The values for ϕ_{corr} in the first data column are "steady-state" values recorded after 24 hours. Corrosion potentials for the composites compare in magnitude, and in most cases exceed the ϕ_{corr} determined for pure graphite. The ϕ^s_{corr} and ϕ^e_{corr} values of GECM samples were taken after a 15-minute pre-test and post-test delay. An average ϕ^s_{corr} and ϕ^e_{corr} are shown for the materials with the corresponding high and low values. The wide variations in the ϕ^s_{corr} values were due to the fact that the GECM did not have sufficient time to equilibrate (24 hours required). Values of ϕ^e_{corr} likewise varied, and was in fact influenced by effects of the prior galvanic coupling.

TABLE 6

OPEN CIRCUIT CORROSION POTENTIAL (ϕ_{corr}) AFTER 24 HOURS IN 3.5% NaCl, CORROSION POTENTIALS BEFORE (ϕ^{s}_{corr}), AND AFTER (ϕ^{e}_{corr}) GALVANIC COUPLE TEST FOR GRAPHITE MATERIALS, 3.5% NaCl, pH7, 22 ± 1°C

Graphite Material	ϕ_{corr} (mv)	ϕ^{s}_{corr} (mv)	ϕ^{e}_{corr} (mv)
3501-5	+ 179	+ 145 high + 9 mean - 221 low	+ 71 high + 5 mean - 235 low
Modmor II	+ 90	+ 4 high - 120 mean - 190 low	+ 4 high - 41 mean - 90 low
T-300	+ 160	+ 4 high - 118 mean - 242 low	+ 5 high - 81 mean - 146 low
Magnamite II	+ 160	+ 80 high + 17 mean - 45 low	- 86 high - 99 mean - 114 low
Pure Graphite	+ 120	+ 120 high + 55 mean - 73 low	+ 96 high + 20 mean - 54 low

2. GALVANIC CURRENT DATA

Values of average galvanic current, $\bar{I}_g$, determined from graphical integration of the time versus I_g plots were then divided by the galvanic reaction surface, (approximately 17 cm^2 for most samples) to obtain average galvanic current density $_g\bar{i}_g$. This value along with the galvanic corrosion rates, r_g, in both mdd and mpy are listed in Tables 7 through 11. Each of these tables ranks the alloy within its alloy type according to its galvanic corrosion susceptibility. Also listed is the couples overall galvanic series ranking. Actual weight loss r_A data is listed for comparison with corrosion rates calculated from $\bar{i}_g$ data. The corrosion potential difference at the start of the

test $\Delta\phi^{s}_{corr}$ is shown as a basis for comparing galvanic current results with corrosion potentials. The following paragraphs treat in detail the alloy types with descriptions of the time - I_g curves along with data presented in the tables indicating galvanic corrosion behavior within alloy series. Table 12 is the overall galvanic series which ranks the alloys according to galvanic current density with those possessing high $\bar{i}_g$ listed first along with actual weight-loss data r_A.

Time vs I_g plots for aluminum alloys indicated that all alloys except aluminum-graphite (alloy-composite) have initial I_g in the 150 to 300 μA range. Al-7075-T6 and Al-2020-T651 reached a steady value and held fairly constant for the entire test period at a higher rate (200-300 μA) than the other Al alloys. Al-2024 (both T3 and T6) and the powder metallurgy (P/M) alloy MA-87 (both in the 72 and 73 forging treatments) initially have a high i_g, that rapidly decreases and stabilizes at a lower rate (150 μA). Aluminum graphite (an advanced composite material) showed a surprisingly low galvanic current (50 μA). The average trends are reflected in Table 7.

TABLE 7

GALVANIC SERIES FOR GECM COUPLED WITH ALUMINUM ALLOYS IN 3.5% NaCl

No.	Coupled To	i_g ($\mu A/cm^2$)	r_g (mdd)	r_g (mpy)	r_A (mpy)	$\Delta\phi^{s}_{corr}$ (mv)	Overall No.
1	2020-T651	17.9	18.6	9.72	13.5	-654	2
2	7075-T6	12.5	12.6	6.5	24.2	-771	5
3	MA-87(73)	10.4	10.7	5.7	30.6	-935	6
4	2024-T6	10.3	10.6	5.6	20.1	-621	8
5	2024-T3	8.7	9.0	4.8	31.2	-703	10
6	MA-87(72)	7.1	7.2	3.9	30.6	-845	12
7	Al-Gr	5.2	4.8	2.8	69.9*	-809	13

*Severe crevice corrosion.

In general, the aluminum alloys had high $\bar{i}_g$ and a correspondingly high r_A and $\Delta\phi^s_{corr}$. The r_A of 2020-T651, an experimental alloy containing lithium and cadmium, was low, whereas $\bar{i}_g$ was high. Al-Gr exhibited atypical behavior by having a very low $\bar{i}_g$ and an extremely high r_A.

Pertinent electrochemical and weight-loss data for steels are listed in Table 8. Time-I curves for all steels tested showed very stable behavior with I_g ranging mostly in the 200 to 300 μA range. Carbon steel (1020) and (4130) tended to have lower I_g than alloy steels with higher total alloying element content such as 4340, 300M, and AF 1410, I_g decreased with time for 1020 and 4130 whereas 4340, 300M, and AF 1410 showed an increase in galvanic current. Table 8 shows an interesting trend. It is observed that the higher alloy content steels have a greater $\bar{i}_g$ than the leaner steels, while actual weight-loss data indicates r_A for 1020, 4130, and 4340 is much greater than 300M or AF 1410. Severe pitting was observed on AF 1410; this makes the interpretation of I_g or r_A data very difficult. In general, the steel alloys had very high $\bar{i}_g$ of about the same magnitude or higher than Al alloys. Note, that $\Delta\phi^s_{corr}$ for steels is somewhat lower than that of Al alloys, which indicates that their galvanic susceptibility should be lower if potential alone was considered.

TABLE 8

GALVANIC SERIES FOR GECM COUPLED WITH STEELS IN 3.5% NaCl

No.	Coupled To	$\bar{i}_g$ (μA/cm^2)	r_g (mdd)	r_g (mpy)	r_A (mpy)	$\Delta\phi^s_{corr}$ (mv)	Overall No.
1	4340	21.7	53.7	9.9	45.5	-608	1
2	300M	17.2	42.7	7.9	5.9	-249	3
3	AF 1410	15.7	38.7	7.1	5.2	-517	4
4	4130	10.4	25.9	4.8	75.1	-523	7
5	1020	9.9	24.7	4.1	53.8	-529	9

*Severe pitting occurred on specimen surface.

For stainless steels, the time vs I_g plots indicated a relatively low magnitude of I_g, but with seemingly inherent instability with time. One stainless steel, SS-440C experienced moderately high I_g. Table 9 shows this rather high $\bar{i}_g$ and the correspondingly high r_A. SS-440C experienced severe pitting. Table 9 indicates that the other stainless steels had low $\bar{i}_g$ and also low r_A. Except for SS-440C, the lower $\Delta\phi^s_{corr}$ indicates that stainless steels are much compatible with GECM, as was indicated by $\bar{i}_g$ data.

Corrosion data for nickel-base or superalloys are listed in Table 10. Time vs i_g curves indicated a rapid decrease in I_g to an almost zero value that remained constant throughout the test period. The i_g values were small, and r_A was negligible. Notice the contrast between the low $\bar{i}_g$ and the relatively large value of $\Delta\phi^s_{corr}$ for nickel alloys. This high potential difference would indicate a higher galvanic corrosion, which proves not to be the case.

TABLE 9

GALVANIC SERIES FOR GECM COUPLED WITH STAINLESS STEELS IN 3.5% NaCl

No.	Coupled To	$\bar{i}_g$ ($\mu A/cm^2$)	r_g (mdd)	r_g (mpy)	r_A (mpy)	$\Delta\phi^s_{corr}$ (mv)	Overall No.
1	SS-440C*	8.18	19.0	3.54	19.87	-298	11
2	SS-301	2.24	5.34	0.98	1.16	-200	14
3	SS-304	1.40	3.26	0.59	nil	-240	16
4	PH 17-7	1.05	2.36	0.44	nil	-233	17
5	AFC-77	1.03	2.32	0.42	nil	-309	18

*Severe pitting occurred on specimen surface.

TABLE 10

GALVANIC SERIES FOR GECM COUPLED WITH NICKEL-BASE ALLOYS IN 3.5% NaCl

No.	Coupled To	i_g ($\mu A/cm^2$)	r_g (mdd)	r_g (mpy)	r_A (mpy)	$\Delta\phi^s_{corr}$ (mv)	Overall No.
1	Inconel	0.435	1.15	0.180	nil	-402	19
2	Inconel X	0.055	0.13	0.023	nil	-255	20
3	Rene´41	0.037	0.08	0.014	nil	-428	21

Titanium alloys indicated Time - I_g behavior similar to that of the nickel-base alloys with an even smaller I_g. Table 11 indicates the excellent galvanic corrosion resistance of titanium alloys. Here again $\Delta\phi^s_{corr}$ would indicate a much higher galvanic corrosion susceptibility if corrosion potentials alone were considered.

Beryllium-copper (Be-Cu) exhibited very stable I_g over the test period. Its $\bar{i}_g$ (Table 11) was in the range of the stainless steels, and it experienced a small r_A. In this case, the small $\Delta\phi^s_{corr}$ did correlate with its low $\bar{i}_g$.

It was further noted that the type of GECM usually had little effect on corrosion rate of the alloys to which it was coupled. This was evident since in numerous cases different types of GECM were used in replicate tests with no apparent effect on producibility. In most cases replicate I_g - Time curves could be superimposed, indicating little discernible difference in average galvanic current.

TABLE 11

GALVANIC SERIES FOR GECM COUPLED WITH TITANIUM ALLOYS AND Be-Cu IN 3.5% NaCl

No.	Coupled To	$\bar{i}_g$ ($\mu A/cm^2$)	r_g (mdd)	r_g (mpy)	r_A (mpy)	$\Delta\phi^s_{corr}$ (mv)	Overall No.
1	Ti-6Al-2Sn-4Zr-2Mo	nil	nil	nil	0.84	-408	22
2	Ti-6Al-4V	nil	nil	nil	0.00	-280	23
-	Be-Cu	1.42	8.06	1.3	1.82	-292	15

SECTION VII

DISCUSSION

1. ALLOY BEHAVIOR

From the results obtained above, some explanations for the observed behavior of the alloy/GECM couples can be made. The following discussion is in relation to the behavior of Al alloys. Mansfeld and coworkers (Reference 4) observed that Al-7075 uncoupled has a lower corrosion rate in 3.5% NaCl than uncoupled A-2024 (uncoupled corrosion rate, r_o, of 0.95 vs 5.24 mdd, respectively). When the two were coupled with a more noble alloy, the Al-7075 alloy had a higher I_g than Al-2024. This behavior was supported by the results of this research. A possible explanation for the I_g of Al-2020-T651 is the lithium and cadmium alloying elements which are active electrochemically. The P/M MA-87 alloy samples may have experienced reduced I_g due to corrosion product buildup on the sample surface which reduced current flow. The reduced I_g of the P/M MA-87 (73) over MA-87 (72) could be due to the larger particle sizes of the MA-87 (72) macrostructure which increased the overall area for galvanic reaction to occur. The high r_A for Al-Gr can possibly be explained by considering that the corrosion susceptibility of this material is increased by the galvanic coupling effect between the graphite fibers and the Al alloy matrix and additionally by the crevice corrosion which occurs at fiber-metal interfaces. These interactions were pointed out by Dull, et al. (Reference 18) for Al-Gr composites in sodium chloride solutions. Similar conclusions were drawn from examination of specimens used in this study. The electrical insulation effect of high corrosion product buildup on Al-Gr surfaces is offered as an explanation for the low I_g observed.

In relation to the observed behavior of steel, Fink & Boyd (Reference 19) found that steels when totally immersed in seawater, corrode uniformly, independent of alloying elements over a wide range of alloy types; in some instances, low-alloy steels evidenced higher rates than those for plain carbon steel. This investigation shows that the r_A of plain carbon 1020 steel and 4130 low-alloy steel were of similar magnitude and that the

surface corrosion was largely uniform. This tightly adherent uniform corrosion product film was felt to be the reason for the occurrence of decreasing I_g with time for these alloys. Steels, 300M and AF 1410 had lower r_A due to higher alloy content. Their surface, however, had nonuniform or localized product buildup. The resulting nonprotective product film did not enable I_g to decrease with time. In fact, there was an increase in I_g with time for 4340, 300M, and AF 1410 steels. An explanation for this increase is that as crevice and pitting corrosion increases on the metal surface, the cathodic area is reduced and the anodic dissolution reaction can proceed with facility as evidenced by the increase in I_g with time. Low-alloy steel 4340 displayed both high r_A and $\bar{i}_g$. Large areas of crevice corrosion were present on the surface accounting for the high r_A. Increasing I_g with time and high $\bar{i}_g$ could be due to the decreasing cathode to anode ratio on the alloy surface.

The unstable nature of the stainless-steels is due to the forming, breaking down, and reforming of passive films. Even with this active-to-passive instability, overall galvanic current was not high. It must be cautioned that stainless steels undergo other forms of corrosion (e.g., pitting) in chloride media that may make these alloys unacceptable for certain applications in spite of the low $\bar{i}_g$ or r_A. The high corrosion rate of SS-440C is not surprising considering the low nickel content in this alloy.

Both nickel-base and titanium alloys have excellent corrosion behavior in neutral NaCl solutions because of the natural protective oxide films that form on the alloy surfaces. The effect of protective surface films on titanium alloys has been discussed by Rosenfeld and coworkers (Reference 11). The TiO_2 (rutile) film forms an electrical barrier which greatly reduces corrosion current. This explains the low $\bar{i}_g$ observed for both nickel-base and titanium alloys.

The Be-Cu alloy contained mostly copper. Its low corrosion rate was due to the nobility of copper. In this case, low potential difference $\Delta\phi^s_{corr}$ did predict the low galvanic corrosion rate.

2. POTENTIAL VS GALVANIC CURRENT FOR GALVANIC CORROSION ESTIMATES

A comparison of the galvanic series based upon potential considerations in Table 5, and that based upon galvanic current density in Table 12 dramatically illustrates the problems that may be encountered when potential difference is used to predict galvanic corrosion. The exceptionally good galvanic corrosion properties of titanium and nickel-base alloys would be overlooked if potential difference alone was the compatibility criterion. Galvanic corrosion reaction rates are controlled by such kinetic factors as Tafel slopes, uncoupled corrosion rates, and in some cases, on the diffusion rate of reacting species through surface films. The galvanic series, based on galvanic current density, listed in Table 12 is a more reliable indicator of the "galvanic effect" since galvanic current represents the absolute increase in dissolution rate due to galvanic coupling.

TABLE 12

GALVANIC SERIES FOR GECM BASED ON AVERAGE CURRENT DENSITY $\bar{i}_g$ IN 3.5% NaCl

Overall Ranking	Coupled To	$\bar{i}_g$ ($\mu A/cm^2$)	r_A (mpy)	Overall Ranking	Coupled To	$\bar{i}_{gcd_2}$ ($\mu A/cm^2$)	r_A (mpy)
1	4340	21.7	45.5	13	Al-Gr	5.20	69.9
2	2020-T651	17.9	13.5	14	SS-301	2.24	1.16
3	300M	17.2	5.9	15	Be-Cu	1.42	1.82
4	AF 1410	15.7	5.2	16	SS-304	1.40	nil
5	7075-T6	12.5	24.2	17	PH 17-7	1.05	nil
6	MA-87(73)	10.4	30.6	18	AFC-77	1.03	nil
7	4130	10.4	75.1	19	Inconel	0.435	nil
8	2024-T6	10.3	20.1	20	Inconel X	0.055	nil
9	1020	9.9	53.8	21	Rene'41	0.037	nil
10	2024-T3	8.7	31.2	22	Ti-6Al-2Sn-4Zr-2Mo	0.001	1.82
11	SS-440C	8.2	19.9	23	Ti-6Al-4V	0.000	nil
12	MA-87(72)	7.1	30.6				

a. Acceptability Criteria

Table 12 lists the alloys according to the magnitude of the average galvanic current density for a 24-hour test period. This table is intended for use only as a qualitative guideline where knowledge of the absolute increase in corrosion rate due to galvanic coupling is the only concern. The alloys tested were arbitrarily classified into three groups. Group I couples are those that exhibited $\bar{i}_g$ less than 5 $\mu A/cm^2$ and are considered acceptable. Group II couples are considered borderline and have values between 5 and 15 $\mu A/cm^2$. Unacceptable couples would be those with average current densities greater than 15 μA. Table 13 lists the alloys according to these criteria.

b. Correlation of Average Galvanic Current Density and Galvanic Corrosion Determined from Weight-Loss Tests

Tables 7 through 11 list the values of galvanic corrosion rate r_g for various alloys calculated from galvanic current densities. It is noted that there is usually a large discrepancy between this value and r_A, the corrosion rate calculated from weight-loss data. This is because r_A, is a sum of both r_g and the uncoupled corrosion rate of the alloy r_o. Mansfeld, et al. (Reference 4), concluded in a study conducted on Al alloy/metal couples that the best correlation between average current density $\bar{i}_g$ and rates determined from weight-loss tests is found through the empirical relation:

$$\bar{i}_g = k\,(r_A - r_o)$$

where k is the experimentally determined correction factor which relates galvanic current measurements to the actual corrosion rate of the anodic half of a galvanic couple in a particular environment. The use of this empirical relationship requires accurate weight-loss data to determine r_A and r_o. Once k is derived, continuous monitoring of galvanic current gives instantaneous galvanic corrosion rates, a considerable advantage over conventional weight-loss tests. No effort was made to apply correction factors in this research since galvanic current measurements provided an acceptable means of ranking alloys for compatibility with GECM.

TABLE 13

ACCEPTABILITY CRITERIA FOR ALLOYS TESTED

GROUP	ALLOY COUPLED TO GECM
I	Ti-6Al-4V
ACCEPTABLE	Ti-6Al-2Sn-4Zr-2Mo
($\bar{i}_g$ < 5uA/cm^2)	Rene'41
	Inconel X
	Inconel
	AFC-77
	PH 17-7
	SS-304
	Be-Cu
	SS-301
II	Al-Gr
BORDERLINE	MA-87(72)
(5μA/cm^2 < $\bar{i}_g$	SS-440C
< 15μA/cm^2)	2024-T3
	1020
	2024-T6
	4130
	MA-87(73)
	7075-T6
III	AF 1410
UNACCEPTABLE	300M
($\bar{i}_g$ > 15μA/cm^2)	2020-T651
	4340

3. GALVANIC CURRENT DATA VS ACCELERATED AND LONG-TERM TESTS ON ACTUAL GECM/ALLOY JOINTS

To further confirm the validity of using galvanic current measurements as a basis for estimating the increase in corrosion rate of alloys due to coupling to GECM; i_g data from this study was qualitatively compared with results from accelerated and long-term corrosion tests on mechanically fastened and adhesively bonded GECM/alloy joints reported by other investigators.

Brown and Coomber (Reference 20) have performed both accelerated and long-term corrosion tests on graphite-epoxy composite/alloy joints mechanically fastened (bolted) and adhesively bonded in salt spray, marine, and industrial environments. The different alloys used included various aircraft aluminum alloys and unalloyed aluminum in the as-received, chromic acid anodized and conversion coated surface conditions, cadmium plated steel, 18-8 stainless steel, and Ti-6Al-4V. Alloys were tested with both painted and unpainted surfaces.

Long-term atmospheric tests were conducted for periods up to four years in industrial and marine environments. Couples between GECM and Al and Al alloys as well as Cd-plated steel showed severe corrosion in all cases regardless of surface treatment except chromate primed and epoxide top-coated specimens which did show marked resistance over the other couples. No corrosion was noted on stainless steel or titanium specimens, even when dry bolted, under any conditions of exposure.

The results of accelerated 3% and 5% NaCl salt spray tests showed similar trends. Painted specimens showed reduced attack as noted for atmospheric tests but corrosion was not completely eliminated.

Adhesively bonded couples did not exhibit corrosion in either long-term or accelerated tests even for aluminum or Cd-plated steel alloys. This was also concluded in an earlier report devoted exclusively to adhesively bonded galvanic couples (Reference 21).

Prince (Reference 22) concluded from salt spray (5% NaCl) tests conducted on Al-2117, Cd-plated steel, A286 steel, MP35N, and Ti-6Al-4V

fasteners with and without various coating systems in contact with GECM that aluminum, Cd-plated steel, and A286 steel were susceptible to galvanic corrosion and that Ti-6Al-4V and multiphase MP35N were highly resistant to attack. It was further noted that the best protective coating system appeared to be zinc chromate pigmented epoxy primer plus strontium chromate pigmented epoxy polyamide primer followed by an aliphatic polyurethane topcoat. Corrosion tests (humidity + exfoliation salt spray) were conducted by Treadway (Reference 23) on GECM/aluminum and titanium alloy lap joints assembled using titanium, A286 steel, Cd-plated steel, and aluminum fasteners in addition to adhesive bonding. The compatibility of GECM/titanium couples was confirmed. It was observed that corrosion of GECM/alloy joints could be minimized by the application of conventional protective systems consisting of organic coatings and sealants. Adhesive-bonded GECM/aluminum joints were susceptible to attack. This conclusion is contrary to results reported by Brown and Coomber discussed previously and points to the need for further work on the corrosion behavior of adhesively bonded couples.

Johnston and coworkers (Reference 6) report a high rate of corrosion for aluminum and steel couples. It was surprising to note, however, that reportedly severe corrosion was detected on the faying surface of Ti-6Al-4V plate mechanically bonded to GECM. This is contrary to the results given by Treadway (Reference 23), Fischer and Deluccia (Reference 15) and Prince (Reference 22), for similar joints under salt spray where no corrosion was detected. Adhesive bonding and the use of sealants and conventional protective coating systems were found to considerably reduce galvanic corrosion.

Comparison of these results with the results of this study clearly shows the agreement between the qualitative ranking of GECM/alloy couples by galvanic current density and estimates of corrosion severity or galvanic compatibility derived from other types of corrosion tests. The compatibility of Ti and some stainless steel alloys or the high corrosion rate for steel and aluminum alloys could have been predicted from $\bar{i}_g$ data. It cannot be overemphasized, however, that these data are useful only for preliminary screening of alloys for susceptibility to galvanic corrosion when coupled with GECM in contact with aqueous chloride containing media.

SECTION VIII

CONCLUSIONS

From the results of this research, the following conclusions are made:

1. Potential difference measurement is a poor indicator of the extent of galvanic corrosion experienced when GECM is coupled with an alloy.

2. Continuous I_g data monitoring gives the time dependent variations in galvanic corrosion rates more readily than conducting weight-loss tests.

3. Compatibility of alloy with GECM were as follows: Steel and aluminum alloys were least compatible. Stainless steels and Be-Cu were better. The best alloys were nickel-base and titanium.

4. The effect of different types of GECM on galvanic corrosion rate is minimal.

5. Galvanic current data were shown to agree with estimates of galvanic compatibility from other experiments, such as salt-spray and long-term atmospheric tests.

The following recommendations are made:

1. Expand the galvanic series by testing other alloys.

2. Perform tests in other media, such as tap water and contaminated hydraulic fluid.

3. Conduct galvanic corrosion tests using protective coatings and sealants.

4. Conduct long-term tests (five days or more) to compare with 24-hour test results.

REFERENCES

1. H. H. Uhlig, Corrosion and Corrosion Control, p. 98, John Wiley & Sons, Inc., New York, (1963).

2. Hercules, Incorporated. Graphite Materials, p. 1.1, Systems Group, Bacchus Works, Magma, Utah, (1975).

3. R. E. Randolph, et al. Graphite Composite Landing Gear Components-Side Brace Assembly and Torque Link for A-37B Aircraft, p. 6, AFFDL-TR-73-69, Wright-Patterson Air Force Base, Ohio, Air Force Flight Dynamics Laboratory, (1973).

4. F. Mansfeld, et al., "Galvanic Corrosion of Al Alloys the Effect of Dissimilar Metal," Corrosion, Vol. 30, p. 343, (1974).

5. P. F. Dexter, Graphite-Epoxy Landing Gear Environmental Tests, p. 33, AFFDL-TM-74-217, Wright-Patterson Air Force Base, (1974).

6. G. R. Johnston, et al. "Galvanic Corrosion Effects Associated with Graphite Composite/Metal Joints," Lockheed Report. LR-26088, The Lockheed Company, Burbank, California, (1973).

7. Military Standard, MIL-STD-889, "Dissimilar Metals".

8. G. Lauer and F. Mansfeld, "Measurement of Galvanic Corrosion Current at Zero External Impedance," Corrosion, Vol. 26, p. 504, (1970).

9. F. Mansfeld, "Area Relationship in Galvanic Corrosion," Corrosion, Vol. 27, p. 436, (1971).

10. W. G. Whitman and R. P. Russell, "The Natural Water Corrosion of Steel in Contact with Copper," Industrial Engineering and Chemistry," Vol. 16, p. 276, (1924).

11. I. L. Rozenfeld, et al. "Some Peculiarities of the Cathodic Behavior of Titanium in Neutral Media," Protection of Metals, Vol. 8, p. 634, (1972).

12. F. Mansfeld and E. P. Parry, "Galvanic Corrosion of Bare and Coated Al Alloys Coupled to Stainless Steel 304 or Ti-6Al-4V," Corrosion Science, Vol. 13, p. 605, (1973).

13. A. R. G. Brown and D. E. Coomber, "Behavior of Couples of Aluminum and Plastics Reinforced with Carbon Fibre in Aqueous Salt Solutions," British Corrosion Journal, Vol. 7, p. 232, (1972).

14. T. P. Hoare, The Electrochemistry of Oxygen, p. 321, Interscience Publishers, Division of John Wiley and Sons, Inc., New York, (1968).

REFERENCES (CONT'D)

15. P. Fischer and T. T. DeLuccia, "Effects of Graphite-Epoxy Composite Materials on the Corrosion Behavior of Aircraft Alloys," Naval Air Development Center, paper presented at the Tri-Service Corrosion Conference, Wright-Patterson Air Force Base, Ohio, (1974).

16. T. Devay, et al. Acta Chemica Hungaria, Vol. 62, p. 157, (1969).

17. T. A. Von Fraunhofer and C. H. Banks, The Potentiostat and Its Applications, p. 35, Butterworths, London, (1972).

18. D. L. Dull, et al. The Corrosion of 6061 Aluminum Alloy Thornel 50 Graphite Composite in Distilled Water and NaCl Solution, SAMSO-TR-75-120, (1975).

19. F. W. Fink and W. K. Boyd, "The Corrosion of Metals in Marine Environments," p. 21, DMIC Report 245, (1970).

20. A. R. G. Brown and O. E. Coomber, Corrosion Risks at Contacts Between Carbon Fibre Reinforced Plastics and Metals," Royal Aircraft Establishment TR-73035, (1973).

21. A. R. G. Brown and D. E. Coomber, The Resistance to Corrosion of Some Insulating Carbon Fibre Reinforced Plastic to Aluminum Alloy Joints, Royal Aircraft Establishment TR-72160, (1972).

22. D. E. Prince, Corrosion Behavior of Metal Fasteners in Graphite-Epoxy Composites, Air Force Materials Laboratory TR-75-53, (1975).

23. D. G. Treadway, Corrosion Control at Graphite/Epoxy-Aluminum and Titanium Interfaces, General Dynamics, Air Force Materials Laboratory TR-74-150, (1974).

☆ U. S. GOVERNMENT PRINTING OFFICE: 1976 — 757-001/143